Pele's hairs and tears: Natural probe of volcanic plume

Séverine Moune [a,*], François Faure [b], Pierre-J. Gauthier [a], Kenneth W.W. Sims [c]

[a] *Laboratoire Magmas et Volcans (OPGC), CNRS— Université Blaise Pascal- IRD, 5 rue Kessler, 63038 Clermont-Ferrand Cedex, France*
[b] *Centre de Recherches Pétrographiques et Géochimiques, CNRS— Universté Henri Poincaré,*
15 rue Notre-Dame des Pauvres, 54501 Vandoeuvre-les-Nancy, France
[c] *Woods Hole Oceanographic Institution, MS #16 Woods Hole, MA 02543, USA*

Abstract

We present a detailed petrographic study of Pele's hairs and tears sampled from Masaya volcano (Nicaragua). This study provides new observations of these little-known pyroclastic objects using both secondary electron images (SEI) and back scattering electron images (BSEI). Our work shows that Pele's tears can be associated with Pele's hairs after their formation: tears can be trapped on the walls and/or in the cavities of Pele's hairs. Moreover, chemical investigations of the Pele's hairs and tears highlight the presence of a chemical zonation. The edge of these tears and hairs show a siliceous enrichment, allowing us to quantify the interaction time of the silicate glass with acid gases in the volcanic plume. This study confirms the syneruptive and post eruptive volatile exsolution from Pele's hairs and tears.
© 2007 Elsevier B.V. All rights reserved.

1. Introduction

Pele's hairs and tears are intriguing pyroclastic products of many basaltic volcanoes: Hawaii, Réunion, Etna (Heiken, 1972; Duffield et al., 1977; Heiken and Wohletz, 1985; Lefèvre et al., 1991; Toutain et al., 1995; Vlastélic et al., 2005; Roeder et al., 2006). Pele's tears are oftentimes found attached to a strand of Pele's hair (Duffield et al., 1977), and Pele's tears and hairs are usually sampled together after an eruptive event. Pele's hairs are a widely distributed clast morphology in sub-marine environments (Clague et al., 2000, 2003). However, Pele's hairs and tears are most typically associated with small subaerial explosive eruptions of low-viscosity ($<10^2$ Pa s) basaltic melts (Heiken and Wohletz, 1985). In many cases, Pele's hairs and tears are formed by deformation of low-viscosity lava in the air. In low-viscosity magmas, droplet shape is controlled by surface tension, acceleration of the droplet after eruption and air friction (Heiken, 1972). Experiments performed by Shimozuru (1994) suggest that Pele's hairs are produced when the spurting velocity of erupting magmas is high and Pele's tears when it is relatively low.

Currently there are few detailed studies of Pele's hairs, and even fewer of Pele's tears (Heiken, 1972; Duffield et al., 1977; Heiken and Wohletz, 1985; Shimozuru, 1994). In this manuscript, we present a detailed petrographic and geochemical study of Pele's hairs and

---

* Corresponding author. Present address: Institute für Mineralogie, Callinstrasse 11, 30165 Hannover, Germany. Tel.: +49 511 762 5662; fax: +49 511 762 3045.
E-mail address: s.moune@mineralogie.uni-hannover.de
(S. Moune).

tears sampled on Masaya volcano (Nicaragua) using both secondary electron images (SEI) and back scattering electron images (BSEI). The main goal of this study is to use our new observations of the Pele's tears and hairs to better understand the small scale eruption dynamics of basaltic systems. We also show that fine scale variations in the chemical composition of these Pele's hairs and tears elucidate the syn- and post eruptive alteration processes occurring as a result of their interaction with the volcanic gas plume.

2. Geological setting

Masaya volcano is a persistently active basaltic shield volcano on the Central American volcanic front, located about 25 km SE of Managua in Nicaragua. The Masaya Complex (600 m above sea level) is a large, shallow and elongated (6–11.5 km) caldera. Since 1853 the currently active crater (Santiago) has been the site of five periods of ephemeral lava lake development, mild strombolian eruptions, intense gas emission, volcanic tremor and inner crater wall collapse (Stoiber and Williams, 1986; Rymer et al., 1998).

The last reactivation of Masaya volcano took place in Santiago crater in mid-1993 (Delmelle et al., 1999) and continues today. This last eruptive cycle has already been studied by many authors (e.g. Horrocks et al., 1999; Burton et al., 2000; Allen et al., 2002; Delmelle et al., 2002; Duffell et al., 2003; Mather et al., 2003) and is characterized by persistent degassing with almost no juvenile magma emissions. However, some Pele's hairs and tears were expelled from its vent, which sometimes exhibits weak incandescence. These Pele's hair and tear samples were collected in November 2003, just after their emission, from inside the Santiago crater near the active vent.

3. Analytical procedures

Pele's hairs and tears (mounted in epoxy and prepared as polished thick or thin sections) were examined using both petrographical and scanning electron microscope (SEM) techniques. SEM work was carried out at "Laboratoire Magmas et Volcans" (LMV, Clermont-Ferrand) on a JEOL 5910LV equipped with an X-ray analyzer (Princeton Gamma-Tech) operating in energy dispersive mode (EDS) and with the SPIRIT software that allows us to measure the size of each tear in the photograph. We used secondary electron detection to observe surface topography of samples, or backscattered electron mode to obtain an image of local variations in average atomic number of the specimen (analytical

conditions are 15 kV accelerating voltage, 2 nA probe current and 19 mm working distance).

Electron microprobe analyses were performed with a Cameca SX-100 at LMV using a beam current of 8 nA, an accelerating voltage of 15 kV. Chemical profiles across glass were performed with a focused beam due to the small size of the analyzed area.

4. Results

4.1. Morphology of Pele's tears and hairs of Masaya volcano

Pele's tears are small spherical pyroclasts (Fig. 1A). Their sizes are variable (from few μm to several hundreds μm of diameter) and their surfaces are generally rough (Fig. 1A). The prevalent roughness on the entire surface of the tear suggests particle–particle interaction during transport within the volcanic plume rather than shock during ground impact. This process of particle interaction has already been suggested by Heiken (1972) to explain similar observations. As described by Heiken and Wohletz (1985) for Pele's tears of Hawaiian volcanoes, small particles adhering to the surface of the Pele's tear of Masaya volcano (Fig. 1A arrows) are also observed, and are interpreted as small particles of basaltic glass or soluble sublimates condensed from gases of the eruptive plume.

Pele's hairs are cylindrical in form (1 to 500 μm in diameter). These thin, long strands of glass (up to 8 mm in this study) are never found complete because they are delicate and break up in the wind or on contact with the ground (Fig. 1B, C; Heiken and Wohletz, 1985). Pele's hairs display multiple vesicles, typically parallel to the axis of elongation. These vesicles can break and often form long open cavities (Fig. 1D). Moreover, particles with irregular form were detected adhering to Pele's hair surfaces (Fig. 1E). These particles have the physical and chemical characteristics typical of volcanic chloride aerosols from the Masaya gas plume (particles rich in Na, K, Ca, Al and especially Cl; Moune et al., 2005). This observation confirms previous studies of Duffield et al. (1977) and Heiken and Wohletz (1985) suggesting that sublimates can adhere to the surface of Pele's hair.

Pele's hairs can form from droplets that are stretched into threads. Hence, hairs are often found with attached droplets, known as Pele's tears, at their end (Fig. 1B; Duffield et al., 1977). During the formation of Pele's hairs some knots can be also formed along their length (Fig. 1B, C). This morphology can be easily explained by the presence of crystals enclosed in the glass that could not stretch and thus formed small knots in the hair (Duffield et al., 1977).
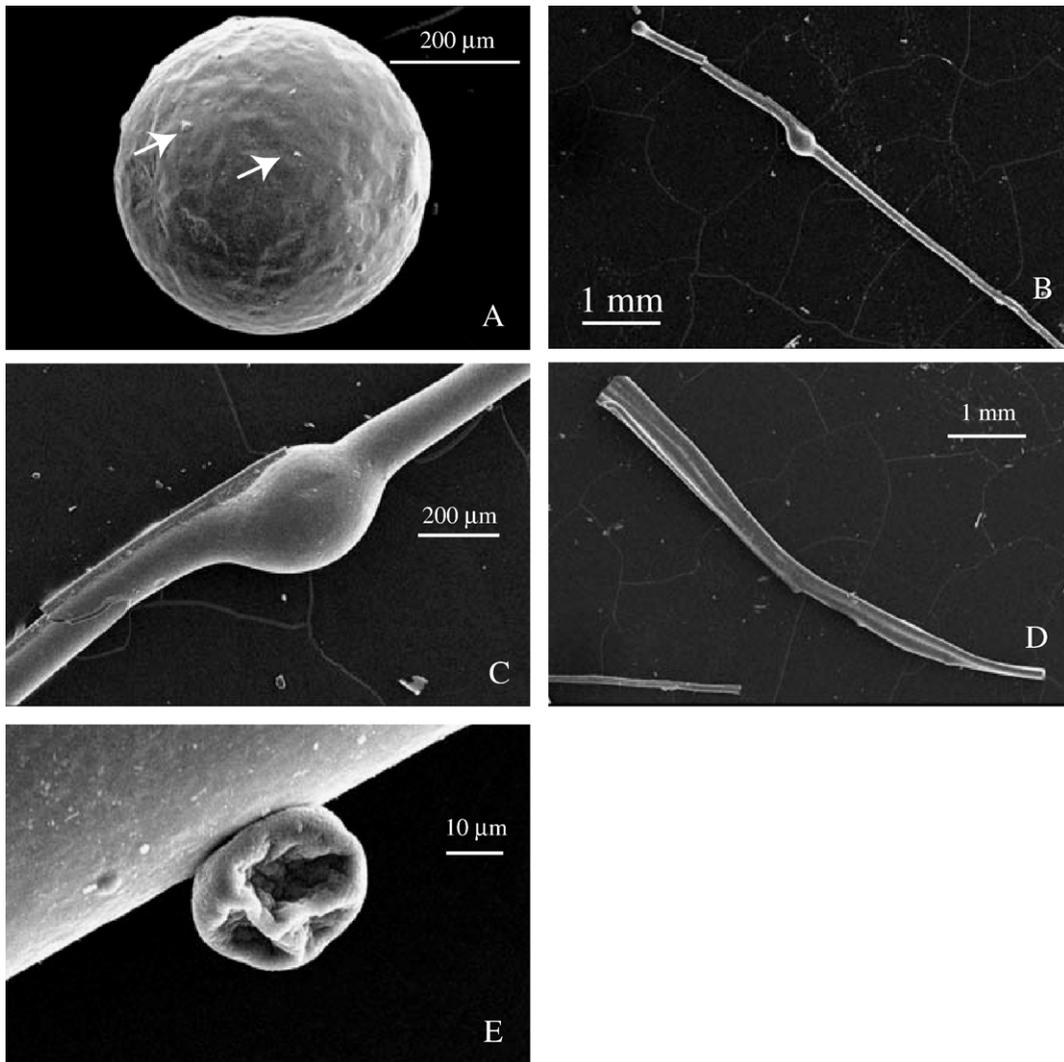
Fig. 1. Morphologies of Pele's hairs and tears from Masaya volcano. A. SEI of a Pele's tear. This spherical basalt pyroclast has a rough surface with small particles adhering to it. B. SEI of a Pele's hair (extremity is broken) associated with a "knot" along the hair and a droplet, known as Pele's tear, at its end. C. Enlargement of a Pele's hair exhibiting a "knot" at a point along its length. This morphology can be easily explained by the presence of crystals enclosed in the glass (see text). D. Pele's hairs displaying long vesicles, open to the outside, that are parallel to their stretching axis. E. Volcanic sublimate of approximately 20 μm of diameter adhering to the surface of a Pele's hair.

Pele's tears are commonly observed on the walls of Pele's hairs and also within cavities of Pele's hairs (Fig. 2A to F). Walls of the cavities are sometimes very thin, easily fractured (Fig. 2C) and tears can be observed through the walls of the cavity (Fig. 2C arrow). Cavities may act like funnels (sampler of tears) during transport of Pele's hairs in the volcanic plume, either during the actual eruption and/or on the crater floor, thus allowing the trapping of the tears in cavities (Fig. 2D). This hypothesis of funnel capture during transport in the volcanic plume seems consistent with the observed concentration of Pele's tears at the bottom of cavities (Fig. 2E). Therefore, it would seem that Pele's tears may be associated with Pele's hairs due to the effects of transport rather than due to common process of formation. Some sublimates (Fig. 2B arrows) can be also observed adhering to the surface of the tears inside these cavities. The second location of variable size Pele's tears is on the walls of Pele's hair, outsides the cavities (Fig. 2F). These droplets are typically concentrated on the surrounding raised edges formed along the external walls of Pele's hairs (Fig. 2F), with these raised edges creating a kind of barrier allowing trapping of the tears. Therefore, as suggested by Fig. 2A to F, it would seem
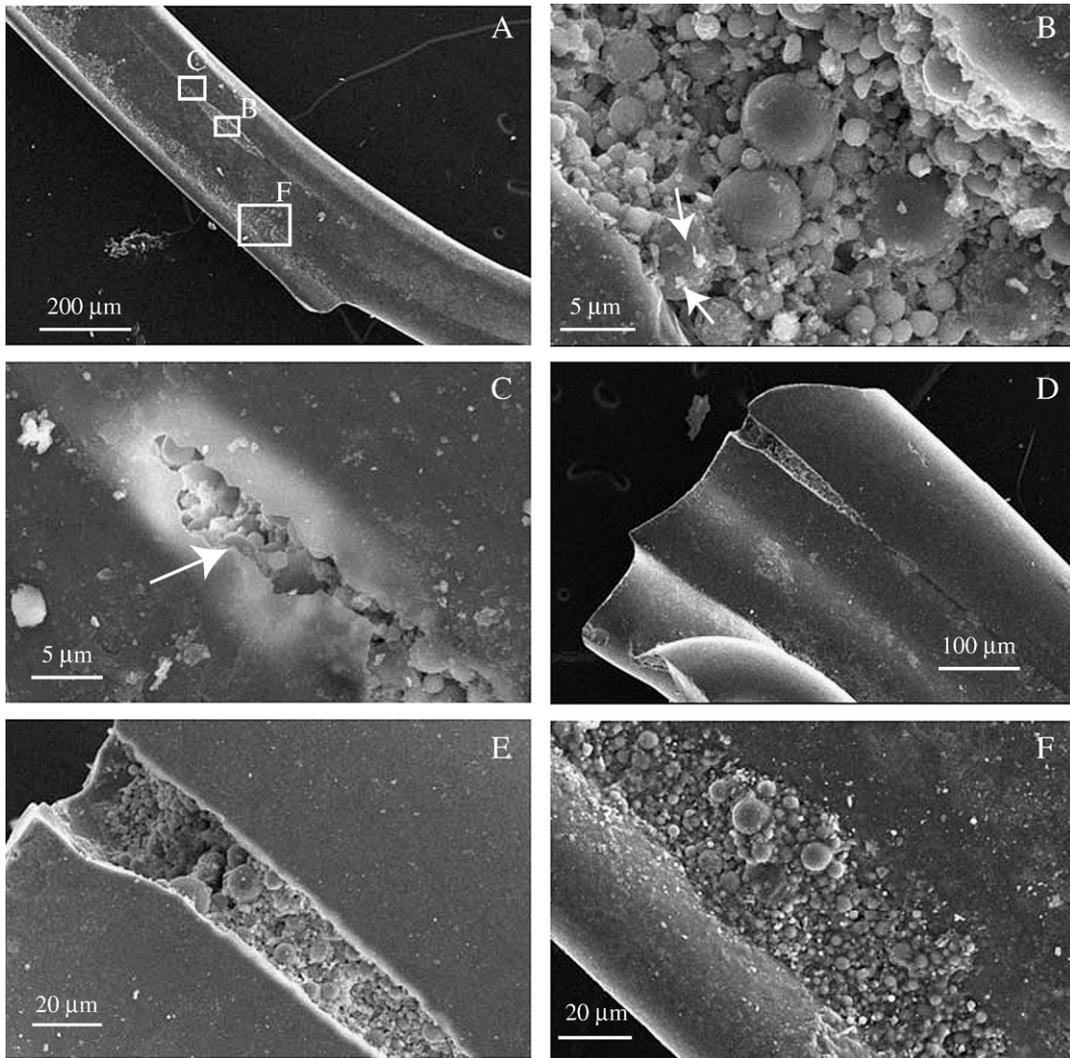
Fig. 2. The different localizations of Pele's tears associated with Pele's hairs, independently from their mechanisms of formation (see text). A. Images of Pele's tears along the walls and within cavities of a Pele's hair. B. Huge quantity of Pele's tears inside a cavity of Pele's hair. The tears have very variable sizes. C. The walls of the vesicle of a Pele's hair are so fine that they are fractured. Therefore they become open cavities towards outside. D. These open cavities of Pele's hair seem to act like funnels during transport of Pele's hairs in the volcanic plume thus allowing the trapping of the tears in cavities. E. Enlargement of D. The concept of funnel entrapment during transport is consistent with the compaction of Pele's tears at the bottom of the cavities. F. Huge quantity of Pele's tears on the surface of the Pele's hair, outside the cavities. The tears have very variable sizes.

that Pele's tears can be associated with Pele's hairs independent of their mechanism of formation (i.e. tears can adhere on the walls and/or be channeled in the cavities of Pele's hairs).

4.2. Cross-section of Pele's tears and hairs of Masaya volcano

Cross-sections across Pele's tears reveal several characteristics not observed in SEI. First spherical gas bubbles are seen in bigger tears (Fig. 3A). Bubbles can be quite large (e.g. Fig. 3A, showing a bubble 150 µm in

diameter within a tear with approximate diameter of 800 µm). Second micro-phenocrysts are sometimes observed inside the glass of the tears. Fig. 3B displays a crystal of plagioclase of "tabular shape" as defined by Lofgren (1971). This crystal appears to be linked to a gas bubble. Finally, cross-sections sometimes reveal a distinct chemical boundary at the tears' periphery (Fig. 3A, B, C). It is important to note that this chemical zonation is present around the entire tear. The maximum thickness of this edge, observed on the whole of the pyroclastic products, is approximately 10 µm. Nevertheless, we note more developed zones associated with fractures (Fig. 3C).
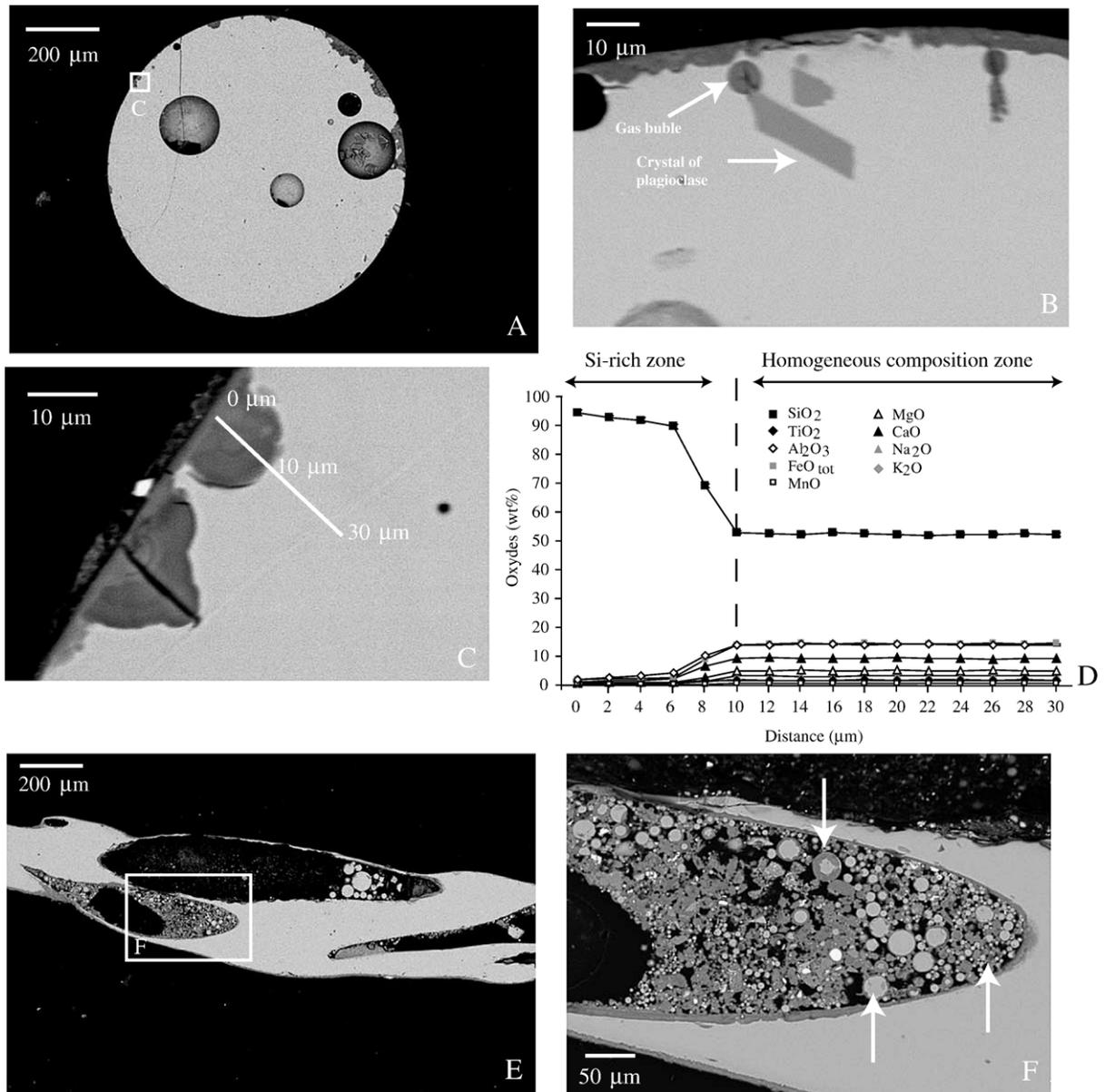
Fig. 3. Cross-sections of Pele's tears and hairs of Masaya volcano. A. BSEI of Pele's tear displaying some spherical gas bubbles. The small darker particles inside the bubbles are material derived from polishing. Note the presence of a chemical variation contrast at the tear's periphery. B. A tabular microcrystal of plagioclase linked to a gas bubble within the glass of a Pele's tear. Note the presence of a chemical variation contrast at the tear's periphery. C. Enlargement of the framed zone in photograph A showing a > 10 μm chemical contrast zone associated with a fracture. D. Compositional profiles along the white feature in C, from the edge towards the interior of the Pele's tear, in increments of 2 μm (see text for discussion). Chemical compositions are in weight% and normalized at 100%. Raw data are given in Table 1. E. Pele's hair with open cavities containing a huge quantity of tears and displaying also chemical zonation both outside and inside the walls of the cavities. F. Enlargement of the framed zone in photograph E highlighting an edge chemically different, around the tears in cavities, on internal walls of the cavities and on outer parts of the hair.

Profiles of chemical composition carried out with the electronic microprobe from the outer to inner parts of the tear (along the white feature on the Fig. 3C, in increments of 2 μm) highlight the presence of a strong chemical gradient in the concentration of major elements, particularly silica (Fig. 3D). Enrichment in silica near the edge is consistent with the strong contrast of this zone in BSE (Fig. 3B, C). Chemical analyses are presented in Table 1. The major-element totals (which should theoretically sum to 100%) are low in the outer zone of the tears by ∼14%. In contrast, the chemical compositions of glass in the inner part of the tears are

Table 1
Variations of chemical composition (in wt.%) of a Pele's tear along a layout, with increments of 2 μm, from outer (0 μm) to inner parts of the tear

Distance (μm)	0	2	4	6	8	10–30
SiO_2	81.7	81.7	81.5	79.1	67.5	50.9 (0.6)
TiO_2	0.84	0.58	0.72	0.71	1.22	1.42 (0.13)
Al_2O_3	1.39	2.19	2.54	3.38	9.87	13.5 (0.4)
FeO^*	1.40	1.67	1.70	2.05	8.55	13.8 (0.4)
MnO	0.01	0.03	0.03	0.03	0.11	0.25 (0.08)
MgO	0.23	0.53	0.58	0.63	2.42	4.67 (0.14)
CaO	0.65	1.20	1.32	1.75	6.03	8.81 (0.30)
Na_2O	0.13	0.18	0.18	0.24	1.06	2.83 (0.18)
K_2O	0.20	0.23	0.23	0.39	0.95	1.39 (0.13)
Sum	86.5	88.3	88.8	88.2	97.7	97.6 (0.8)

From 10 μm to 30 μm the average value and its standard deviation (2σ) are given since the compositions are invariant. The sums of the analyses (86 to 88 wt.%) performed in the outer zone of the tears are likely due to high volatile content in the glass suggesting that Masaya melt forming Pele's hairs and tears was not totally degassed at the eruption time (see text for further explanation).

homogeneous and with much higher analytical total of 97–98%. This systematic variation in major-element totals from the tears exterior to its interior is observed for all of the tears analyzed in this study (large tears and spherules in cavities, see below). Moreover, this deficit in major element totals increases systematically with increasing silica enrichment and decreases when all other element concentrations increase. Therefore, we conclude that this variation is not an analytical artifact but indicates a systematic chemical variability from the tears' interior to its rim.

Pele's hairs also exhibit euhedral plagioclase crystals and chemical zonation around the external part of the hairs. In addition, the previously mentioned open cavities along the hairs (Fig. 2C, D) also display chemical zonation on their internal walls (Fig. 3F). The thickness of this dark edge representing silica enrichment is relatively constant on one hair both outside and inside cavity walls. These cavities also contain numerous small tears that also exhibit variable extents of chemical zonation (Fig. 3F). Indeed, some tears do not have chemical zonation, others show edges of variable thicknesses while others are completely transformed (Fig. 3F arrows). The thickness of this edge does not seem related to the size of the tears, suggesting that it is related to plume exposure history. On the other hand, small tears inside the hairs sometimes display fractures but lack evidence of deformation,
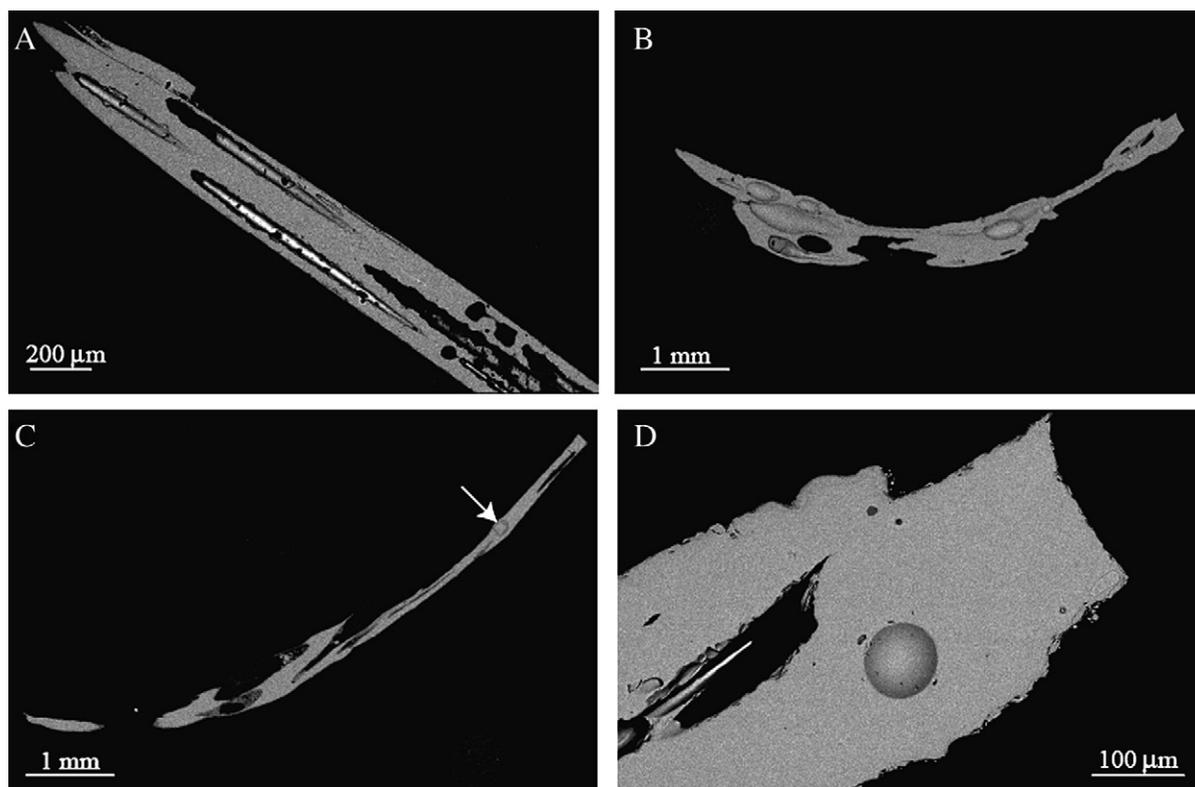
Fig. 4. Shapes of vesicles of Pele's hair. A. Pele's hair displaying elongated vesicles. B. Pele's hair displaying bent vesicles. C. Pele's hair displaying elongated, bent and spherical vesicles. D. Enlargement of the framed zone in photograph C supporting the spherical shape of the vesicle inside the Pele's hair.

suggesting that they had quenched prior to entrapment inside the Pele's hairs.

Observation of along-axis sections of Pele's hairs shows that vesicles inside the hairs are not always elongated parallel to the hair axis but can also be spherical or curved (Fig. 4A–D). These various vesicle shapes are sometimes observed on the same Pele's hair (Fig. 4C), suggesting a complex history of Pele's hair formation. Indeed, these morphologies are not without pointing out the textural characteristics of tube pumice which are known to provide constraints on eruptive dynamics (e.g. Marti et al., 1999; Polacci et al., 2001).

5. Discussion

5.1. Origin of the chemical zonation rim

The gradient in silica concentration observed on the external surface on both Pele's tears and hairs can be explained by two different models:

(1) alteration of the silicate glass by rain water and condensation
(2) dissolution of silicate glass during interaction with volcanic gases in the plume.

Alteration by rain water and atmospheric condensation is not likely, given that our samples were collected within the crater immediately after their eruption. Indeed, the thicknesses of chemical zoning observed on the surface of Pele's hairs and tears (except the zones associated with fractures) would imply interactions between silicate glass and basic pH water for lengths of time from several months and several years (Gislason et al., 1992; Techer et al., 2001). Moreover glass altered by water would display an enrichment in Si (as observed), but also an enrichment in Al and Ti due to different mobility of network forming cations relative to network modifying cations: K, Na, Ca, Mg (Sterpenich and Libourel, 2001). However, in Pele's tears, Al and Ti show a similar behavior to the other network modifying cations. Therefore weathering phenomena can be refuted because the chemical compositions of Pele's tears and hairs are distinctly different than predicted by glass-leaching experiments.

The second and most viable mechanism to explain the compositional rims in the Pele's tears and hairs is the interaction of silicate glass with the acidic gases in the volcanic plume. These samples were collected inside the Santiago crater suggesting that they were exposed to the concentrated volcanic gas plume of Masaya volcano. The experimental study by Spadaro et al. (2002) shows that alteration of basaltic glasses by cold volcanic gases ($T < 10\ °C$) occurs over a very short time period and becomes significant within a few hours of exposure. This alteration leaches almost all the major elements, resulting in enrichment of Si (Fig. 3D) and can rapidly form pure silica when taken to completion (e.g Spadaro et al., 2002). Volcanic glass hydrates rapidly when exposed to acidic gases (Yanagisawa et al., 1997; Spadaro et al., 2002). In fact, a hydration layer is detectable within 1 h of exposure (Spadaro et al., 2002). Yanagisawa et al. (1997) also noted a hydration layer, during dissolution processes. Thus we infer that the low glass totals in the tears' rim are due to high volatile contents in the glass, hypothesis consistent with their exposure to the acidic gas of the Masaya (Horrocks et al., 1999; Burton et al., 2000). Because the volcanic vapor is dominated by H_2O with minor abundances of CO_2, SO_2, HCl, and HF (e.g. Burton et al., 2000) alteration process within the eruptive plume can also explain the presence of the Si-enriched zones, including in the cavities of the Pele's hairs if they are opened outward and hence exposed to the acidic plume.

The morphological irregularity of the chemical zonation (e.g. Fig. 3A–C–F) is also consistent with dissolution of glasses by volcanic gases rather than an alteration by rain water (e.g. Sterpenich and Libourel, 2001; Spadaro et al., 2002). Furthermore, our hypothesis also explains the variations in thickness of the siliceous edges, including the size variation of the siliceous edges on the microsphérules, associated with Pele's hairs. Because the observed chemical variations can be explained by variable residence times of Pele's tears within the volcanic plume, before their entrapment on the walls and/or in cavities of Pele's hairs, quantification of the kinetics of siliceous edge formation may potentially yield a chronometer for pyroclastic residence time within the plume. Indeed, experimental studies suggest that the microsphérules with no chemical zonation were exposed to volcanic gases for less than 4 h; the maximum thickness and Si enrichment of the altered zone (10 μm and ~ 90 wt.%, respectively) was probably reached after five days of exposure. Beyond 5 days, the thickness and concentration in Si are thus no longer a potential marker of the interaction time of the silicate products with the volcanic plume, either during the actual eruption and/or on the crater floor. It is important to note that, at Masaya, low saturated vapor pressure of water at night results in strong condensation of plume water vapor (Burton et al., 2001). Thus this acidic volcanic water condensation could enhance and speed up this alteration process at night. However, in the present case, an exposition as long as 5 days within the

volcanic plume seems unlikely as dense pyroclastic products probably fall down to the ground faster than that. Although Pele's hairs and tears were collected shortly after they had settled to the ground (some of them being collected at the very time of their deposition), some of them might have been a few hours to days old and might have undergone significant gas exposure after they deposited on the crater floor. Alternatively, it cannot be ruled out that some of the alteration also takes place after the sampling of particles on the crater floor if they were coated with acidic condensates. This suggests that, in order to really get at the dynamics in the plume, one requires collecting Pele's hairs and tears as they fall to the ground and not particles that have been on the ground even for short time.

Because huge variations of chemical compositions (SiO_2 ranging from 48 to 90 wt.%) have also been measured in microspherules collected in various other volcanic plumes (Etna, Lefèvre et al., 1985; Toutain et al., 1995; Hawaii, Lefèvre et al., 1991), we believe that this unique alteration signal has potential as a qualitative and even possibly quantitative measure of residence time of Pele's hairs and tears within the volcanic plume.

5.2. Thermal history of the Pele's tears and hairs: implications for the dynamic of eruption

Pele's tears and hairs are essentially composed of glass which infers rapid cooling in the eruptive plume. Presence of euhedral plagioclase crystals in this glass indicates that Masaya magma was not super-heated at the time of eruption and that cooling was rapid as these crystals do not display dendritic overgrowths. We conclude that both hairs and tears were quenched rapidly. Absence of devitrification textures, like spherulites, indicates that the plume temperature was below the glass transition temperature, and no reheating occurred during or after the transport of the pyroclastic materials in the plume (Lofgren, 1971). Indeed, recent experimental studies show that crystal growth can be very rapid for thermal conditions near the glass transition as this allows for dendritic growth all around the rim of the silicate bead (Roskosz et al., 2005). This rapid quenching is consistent with the impact tracks observed on all of the tears exterior surfaces, which are interpreted to be a result of collision between particles during plume transport.

Presence of vesicles inside bigger tears suggests that the Masaya magma was not totally degassed at the time of eruption. This inferred presence of volatiles is consistent with chemical analysis performed in glass of the Pele's tears that always shows, by the "difference method" (Devine et al., 1984), a concentration of volatiles (probably H_2O) between 2.9 and 1.9 wt.%. Electron microprobe analysis (Mather et al., 2003, 2006) of matrix glass from Pele's hairs of Masaya volcano in 2001 and 2003 show similarly low totals of 2.1 and 1.3 wt.% respectively.

Presence of vesicles suggests a rapid exsolution of gas at the eruption time. Various shapes of the vesicles allow us to propose a relative chronology of the eruption; some Pele's hairs display elongated (Fig. 4A, C), bent (Fig. 4B, C) and spherical vesicles (Fig 4C, D). Equilibrium morphology of vesicles inside a silicate liquid is spherical. Therefore the observed elongated and bent vesicles observed imply a two-step process: first nucleation and formation of spherical bubbles and then subsequent deformation of these vesicles. This deformation could have resulted from stretching of lava at the time of extrusion, which is consistent with the general shape of the Pele's hairs. Therefore, by inference the spherical vesicles observed in the stretched out Pele's hairs containing elongated vesicles, must have formed after deformation during eruption. This "second exsolution event" that produced the spherical vesicles must have occurred rapidly as there is considerable evidence that Pele's hairs were quickly quenched (e.g. absence of overgrowth on crystal already present in the basaltic liquid etc.). On the other hand, it is important to note that only spherical shaped vesicles are observed in the Pele's tears (Fig. 3A). This latter observation suggests that no stretching is associated with the formation of Pele's tears. This result is consistent with the Shimozuru's (1994) model, which proposes that Pele's hairs are produced when the spurting velocity of erupting magma is high, and Pele's tears when it is low.

All of our above observations can be explained if the scenario described below is considered. First, Pele' hairs are produced when spurting velocity is high at the top of the magmatic conduit. Vesicles previously formed will be deformed, elongated or curved as a function of location of hair with regard to direction of magmatic gas jets. Secondly, immediately after the extrusion step, spurting velocity decreases but the temperature remains high enough to keep the forming hair liquid. Gas exsolution continues at this step and produces spherical vesicles. At this same time Pele's tears are produced because these pyroclastic materials display only spherical vesicles. The third step corresponds to turbulent motion inside of the eruptive plume where the temperature must be relatively low because no devitrification textures are observed.

Recent studies have highlighted the presence and the role played by syneruptive volatile exsolution during fire fountains episode, and suggested that the dynamics of eruption are determined by a combination of foam collapse at the roof of the magma reservoir and the syneruptive nucleation of bubbles in the annulus of liquid surrounding the ascending gas core (Polacci et al., 2006). Our study of vesicle geometry in the Pele's hairs and tears confirms the occurrence of syneruptive volatile exsolution during the eruptive episode, and provides evidence that the exsolution of gas is efficient even after extrusion of the magma.

6. Conclusion

This detailed petrographic study of Pele's hairs and tears, sampled on Masaya volcano, provides new observations of these little-known pyroclastic materials allowing us to constrain the dynamics of their eruptive process.

This work shows that Pele's tears can be associated with Pele's hairs after their formation; this is clearly evidenced by the observation of tears trapped on the walls and/or in the cavities of Pele's hairs. This entrapment of tears with solids precipitated from volatile phases is important since this phenomenon can modify the impact of volcanic emissions on the chemistry of the atmosphere (aerosols being trapped by Pele's hairs will have a weaker dispersion in the environment) and modify the chemistry of the volcanic plume itself (aerosols, gas and silicate particles trapped can interact between them, enriching the plume in refractory elements, as previously demonstrated by Moune et al., 2006).

The rim of chemical zonation observed in Pele's hairs and tears is best explained by interaction of silicate glass with acidic gases in the volcanic plume and the quantification of the kinetics of the development of this siliceous edge is a potentially important chronometer of the residence time of the pyroclastic products in the plume.

Finally, analysis of vesicle morphology in the Pele's tears and hairs allows us to confirm the occurrence of syneruptive volatile exsolution and provides evidence that this gas exsolution is efficient even after magma extrusion.

Acknowledgements

References

Allen, A.G., Oppenheimer, C., Ferm, M., Baxter, P.J., Horrocks, L.A., Galle, B., McGonigle, A.J.S., Duffell, H.J., 2002. Primary sulfate aerosols and associated emissions from Masaya volcano, Nicaragua. Journal of Geophysical Research 107, 4682.

Burton, M.R., Oppenheimer, C., Horrocks, L.A., Francis, P.W., 2000. Remote sensing of CO_2 and H_2O emission rates from Masaya volcano, Nicaragua. Geology 28, 915–918.

Burton, M.R., Oppenheimer, C., Horrocks, L.A., Francis, P.W., 2001. Diurnal changes in volcanic plume chemistry observed by lunar and solar occultation spectroscopy. Geophysical Research Letters 28, 843–846.

Clague, D.A., Davis, A.S., Bischoff, J.L., Dixon, J.E., Geyer, R., 2000. Lava bubble-wall fragments formed by submarine hydrovolcanic explosions on Loihi Seamount and Kilauea Volcano. Bulletin of Volcanology 61, 437–449.

Clague, D.A., Davis, A.S., Dixon, J.E., 2003. Submarine strombolian eruptions on the Gorda mid-ocean ridge. In: White, J.D.L., Smellie, J.L., Clague, D.A. (Eds.), Explosive Subaqueous Volcanism. Geophysical Monograph, vol. 140. American Geophysical Union, pp. 111–128.

Delmelle, P., Baxter, P.J., Baulieu, A., Burton, M., Francis, P., Garcia-Alvarez, J., Horrocks, L.A., Navarro, M., Oppenheimer, C., Rothery, D., Rymer, H., St-Amand, K., Stix, J., Strauch, W., Williams-Jones, G., 1999. Origin, effects of Masaya volcano's continued unrest probed in Nicaragua. Eos, Transactions of the American Geophysical Union 80, 575–581.

Delmelle, P., Stix, J., Baxter, P.J., Garcia-Alvarez, J., Barquero, J., 2002. Atmospheric dispersion, environmental effects and potential health hazard associated with the low-altitude gas plume of Masaya volcano, Nicaragua. Bulletin of Volcanology 64, 423–434.

Devine, J.D., Sigurdsson, H., Davis, A.N., Self, S., 1984. Estimates of sulfur and chlorine yield to the atmosphere from volcanic eruptions and potential climatic effects. Journal of Geophysical Research 89, 6309–6325.

Duffell, H.J., Oppenheimer, C., Pyle, D.M., Galle, B., McGonigle, A.J.S., Burton, M.R., 2003. Changes in gas composition prior to a minor explosive eruption at Masaya volcano, Nicaragua. Journal of Volcanology and Geothermal Research 2640, 1–13.

Duffield, W.A., Gibson, E.K., Heiken, G., 1977. Some characteristics of Pele's hair. Journal Research US Geological Survey 5, 93–101.

Gislason, S.R., Veblen, D.R., Livi, K.J.T., 1992. Experimental meteoric water–basalt interactions: characterization and interpretation of alteration products. Geochimica et Cosmochimica Acta 57, 1459–1471.

Heiken, G., 1972. Morphology and petrography of volcanic ashes. Geological Society of American Bulletin 83, 1961–1988.

Heiken, G., Wohletz, K., 1985. Volcanic Ash. University of California press, Berkeley, California, p. 245.

Horrocks, L., Burton, M., Francis, P., Oppenheimer, C., 1999. Stable gas plume composition measured by OP-FTIR spectroscopy at Masaya Volcano, Nicaragua, 1998–1999. Geophysical Research Letters 26, 3497–3500.

Lefèvre, R.A., Gaudichet, A., Billon-Galland, M.A., 1985. Emission de microparticules silicatées dans l'atmosphère méditerranéenne par le panache permanent de l'Etna en activité modérée. Comptes Rendus de l'Académie des Sciences 301, 1433–1438.

Lefèvre, R.A., Gaudichet, A., Le Guern, F., 1991. Présence de microsphérules chimiquement variées dans les aérosols de certaines fontaines de lave d'Hawaï. Comparaison avec l'Etna. Comptes Rendus de l'Académie des Sciences 313, 105–111.

Lofgren, G., 1971. Devitrified glass fragments from Apollo 11 and Apollo 12 lunar samples. Proceeding of the Second Lunar Science Conference, vol. 1, pp. 949–955.

Mather, T.A., Allen, A.G., Oppenheimer, C., Pyle, D.M., McGonigle, A.J.S., 2003. Size-resolved characterisation of soluble ions in the particles in the tropospheric plume of Masaya volcano, Nicaragua: origins and plume processing. Journal of Atmospheric Chemistry 46, 207–237.

Mather, T.A., Pyle, D.M., Tsanev, V.I., McGonigle, A.J.S., Oppenheimer, C., Allen, A.G., 2006. A reassessment of current volcanic emissions from the Central American arc with specific examples from Nicaragua. Journal of Volcanology and Geothermal Research 149, 297–311.

Marti, J., Soriano, C., Dingwell, D.B., 1999. Tubes pumices as strain markers of the ductile–brittle transition during magma fragmentation. Nature 402, 650–653.

Moune, S., Gauthier, P.J., Delmelle, P., Sigmarsson, O., 2005. Long-term degassing (1993–2001) of trace elements at an active basaltic volcano: Masaya (Nicaragua). EGU, Vienna, Austria.

Moune, S., Gauthier, P.J., Gislason, S.R., Sigmarsson, O., 2006. Trace element degassing and enrichment in the eruptive plume of Hekla volcano (Iceland) during the 2000 eruption. Geochimica et Cosmochimica Acta 70, 461–479.

Polacci, M., Papale, P., Rosi, M., 2001. Textural heterogeneities in pumices from the climatic eruption of Mount Pinatubo, 15 June 1991, and implications for magma ascent dynamics. Bulletin of Volcanology 63, 83–97.

Polacci, M., Corsaro, R.A., Andronico, D., 2006. Coupled textural and compositional characterization of basaltic scoria: insights into the transition from Strombolian to fire fountain activity at Mount Etna, Italy. Geology 34, 201–204.

Roeder, P., Gofton, E., Thornber, C., 2006. Cotectic proportions of olivine and spinel in olivine–tholeiitic basalt and evaluation of pre-eruptive processes. Journal of Petrology 47, 883–900.

Roskosz, M., Toplis, M.J., Richet, P., 2005. Experimental determination of crystal growth rates in highly supercooled aluminosilicate liquids: implications for rate-controlling processes. American Mineralogist 90, 1146–1156.

Rymer, H., van Wyk de Vries, B., Stix, J., Williams-Jones, G., 1998. Pit crater structure and processes governing persistent activity at Masaya volcano, Nicaragua. Bulletin of Volcanology 59, 345–355.

Shimozuru, D., 1994. Physical parameters governing the formation of Pele's hair and tears. Bulletin of Volcanology 56, 217–219.

Spadaro, F., Lefèvre, R.A., Ausset, P., 2002. Experimental rapid alteration of basaltic glass: implications for the origins of atmospheric particulates. Geology 30, 671–674.

Sterpenich, J., Libourel, G., 2001. Using stained glass windows to understand the durability of toxic waste matrices. Chemical Geology 174, 181–193.

Stoiber, R.E., Williams, S.N., 1986. Sulfur and halogen gases at Masaya caldera complex, Nicaragua: total flux and variations with time. Journal of Geophysical Research 91, 12215–12231.

Techer, I., Advocat, T., Lancelot, J., Liotard, J.M., 2001. Dissolution kinetics of basaltic glasses: control by solution chemistry and protective effect of the alteration film. Chemical Geology 176, 235–263.

Toutain, J.P., Quisefit, J.P., Briole, P., Aloupogiannis, P., Blanc, P., Robaye, G., 1995. Mineralogy and chemistry of solid aerosols emitted from Mount Etna. Geochemical Journal 29, 163–173.

Vlastélic, I., Staudacher, T., Semet, M., 2005. Rapid change of lava composition from 1998 to 2002 at Piton de la Fournaise (Réunion), Inferred from Pb isotopes and trace elements: evidence for variable crustal contamination. Journal of Petrology 46, 79–107.

Yanagisawa, N., Fujimoto, K., Nakashima, S., Kurata, Y., Sanada, N., 1997. Micro FT-IR study of the hydration-layer during dissolution of silica glass. Geochimica et Cosmochimica Acta 61, 1165–1170.